Antigen-Presenting Cell Population Dynamics during Murine Silicosis

Celine A Beamer[1] and Andrij Holian[1]

[1]Center for Environmental Health Sciences, Department of Biomedical and Pharmaceutical Sciences, University of Montana, Missoula, Montana

Silicosis is an occupational lung disease resulting from the inhalation of silica particles over prolonged periods of time, which causes chronic inflammation and progressive pulmonary fibrosis. Alveolar macrophages (AM) are critical effector cells, while less is known about the role and function of pulmonary dendritic cells (DC) in silicosis. We hypothesize that a balance exists between the suppressive nature of AM and the stimulatory capacity of DC to regulate lung immunity, and that this equilibrium may be overcome by silica exposure *in vivo*. Our results demonstrate that in response to silica exposure, both the percent and absolute number of AM significantly decreased over time, with a concomitant significant increase in DC. Both AM and DC exhibited cellular activation in response to silica, indicated by increased expression of cell surface markers. In the absence of silica-induced AM apoptosis (TNFR 1/2–null and Gld mice), no change was observed in the percent or absolute number of either cell type. Furthermore, bone marrow–derived DC, but not bone marrow–derived macrophages, migrated from the alveoli into the lung parenchyma in response to silica, resulting in significantly increased numbers of activated T lymphocytes. Collectively, the results demonstrate that AM and DC are distinct antigen-presenting cells within the respiratory tract that respond to silica exposure *in vivo* in unique ways, with significant implications for immune reactivity of the lung in response to environmental pathogens.

Keywords: alveolar macrophage; pulmonary dendritic cell; silica; activation; inflammation

CLINICAL RELEVANCE

Little is known about the role and function of dendritic cells (DC) in silicosis. Our results show that DC respond to silica in unique ways, suggesting a previously unrecognized role in the immune reactivity of the lung to environmental particles.

Intrapulmonary deposition of silica results in a granulomatous inflammatory response that progresses to interstitial fibrosis, as well as systemic immune deficits (1–4). Although significant efforts have been made through industrial hygiene standards to control ambient exposures, silicosis remains a prevalent health problem, particularly in developing nations. In addition to its importance as an occupational lung disease, silicosis serves as an experimental platform for understanding the mechanisms involved in lung injury, inflammation, and fibrosis. While the anatomical consequences to silica exposure have been well characterized, the underlying cellular and molecular mechanisms leading to immunopathologic changes remain elusive.

The respiratory tract contains well-defined populations of macrophages and dendritic cells (DC), which are thought to play opposing roles in the development and maintenance of inflammation (5–7). Of these, alveolar macrophages (AM) are avidly phagocytic and readily ingest airborne particulate matter, bacteria, and viruses through various pattern recognition receptors (8, 9). These stimuli may then result in cytokine and chemokine secretion that promotes recruitment of inflammatory cells, immune activation, and deposition of extracellular matrices (10). Phagocytosis of silica results in AM apoptosis and necrosis, with subsequent release of intracellular silica that may become involved in multiple ingestion–re-ingestion cycles, which perpetuates the disease process (11, 12). Resident AM play a prominent role in regulating respiratory immunity by promoting a suppressive environment that limits initiation of immunity (13, 14). Overall, AM function poorly as accessory cells and release factors that suppress adaptive immunity through effects on lymphocyte activation, as well as the antigen-presenting capacity and activation of nearby pulmonary DC (14–19). AM are located in close proximity (0.2–1.0 μm) to DC, such that suppressive factors released by AM need only diffuse across small distances to down-regulate DC *in vivo* (5).

A balance exists between suppressive resident AM and stimulatory pulmonary DC to regulate respiratory immunity (7, 20). Although previous studies suggested that AM migrate and transport antigen from the alveolar space into the draining lymph nodes (LN) (21, 22), others demonstrated that AM depletion *in vivo* augments pulmonary immune responses (13, 23), suggesting that another antigen-presenting cell (APC) induces lymphocyte responses *in vivo* (17). Elimination of AM *in vivo* by clodronate treatment facilitates inflammatory reactions to otherwise harmless airborne particulate and soluble antigens (5, 13, 24). During this process, the proportion of DC increases while the proportion of AM concurrently decreases (7, 25). Silica results in prominent recruitment of immune cells from the periphery which transforms the cellular composition of the alveolar spaces away from suppression and toward inflammation (25). Furthermore, exposure to silica particles of respirable size (< 10 μm) stimulates both the activation and destruction of AM through apoptotic mechanisms (26, 27). In the event of AM depletion after silica exposure, pulmonary DC may encounter antigen, migrate to the draining LN, and stimulate lymphocyte interactions. Given the association between inflammation and lymphocyte-mediated responses due to airborne particulates, DC-mediated immune activation may play a greater role than previously recognized within the respiratory response to environmental contaminants.

Despite the importance of both APC subsets to respiratory immunity, to our knowledge no previous study has specifically examined both AM and DC within the same response *in vivo*, making conclusions about comparative behavior difficult. We hypothesize that the ratio of suppressive AM to stimulatory DC within the alveoli is significantly altered by exposure to crystalline

(*Received in original form March 20, 2007 and in final form June 29, 2007*)

This work was supported by NIH grants ES-015294 (to A.H.), COBRE P20 RR17670 from the National Center for Research Resources (NCRR), and NRSA fellowship ES-013044 (to C.A.B.).

Correspondence and requests for reprints should be addressed to Celine Ann Beamer, Ph.D., Center for Environmental Health Sciences, Dept. of Biomedical and Pharmaceutical Sciences, School of Pharmacy and Allied Health Sciences, 32 Campus Drive, Skaggs Building Room 155, University of Montana, Missoula, MT 59812-1552. E-mail: celine.beamer@umontana.edu

Am J Respir Cell Mol Biol Vol 37. pp 729–738, 2007
Originally Published in Press as DOI: 10.1165/rcmb.2007-0099OC on July 19, 2007
Internet address: www.atsjournals.org

silica, thereby skewing innate and adaptive APC populations and contributing to subsequent inflammation and fibrosis. In the present study, the relationship between pulmonary APC subsets *in vivo* was examined in a murine model of silicosis. AM and DC were defined phenotypically within the alveoli of naïve mice and their response to crystalline silica was characterized. The initial inflammatory response and its subsequent resolution were associated with a depletion of AM and an influx of DC, which returned to equilibrium by 28 days after silica exposure. Furthermore, to clarify the contributions of AM versus DC to the immune response to crystalline silica *in vivo*, the cellular phenotype, activation, and function were examined.

MATERIALS AND METHODS

Mice

Original breeding pairs of C57Bl/6, CD45.1, TNFR 1/2–null, and Gld mice purchased from The Jackson Laboratory (Bar Harbor, ME) were maintained in microisolator units in the University of Montana specific pathogen–free (SPF) laboratory animal facility. Cages, bedding, and food were sterilized by autoclaving, and mice were handled with aseptic gloves at all times. Mice were allowed food and water *ad libitum* and experiments were initiated at 6 to 8 weeks of age. All animal use procedures were in accordance with NIH and University of Montana IACUC guidelines.

Experimental Instillations

Silica (Min-U-Sil-5, average particle size 1.5–2 μm) obtained from Pennsylvania Glass Sand Corporation (Pittsburgh, PA) was acid washed, dried, and determined to be free of endotoxin by Limulus assay (data not shown) (Cambrex, Walkersville, MD). Titanium dioxide was purchased from Fischer Scientific (Houston, TX). Particulates were re-suspended in sterile saline and sonicated for 1 minute before intranasal instillation. C57Bl/6, TNFR 1/2–null, and Gld mice at 6 to 8 weeks of age were anesthetized with ketamine (80 mg/kg) and instilled intranasally with either 25 μl of sterile saline, 1 mg crystalline silica, or 0.5 mg titanium dioxide (nonfibrogenic particle control at same surface area) suspended in 25 μl of sterile saline. Mice were returned to their cages and monitored until mobility returned.

Lavage Cell Recovery and Flow Cytometry

Naïve C57Bl/6 mice and at 1, 3, 7, and 28 days after saline, silica, or titanium dioxide instillation (n = 4–6, in duplicate or triplicate), mice were anesthetized with Euthasol (Med-Pharmex Inc., Pomona, CA) the tracheas cannulated, and cells harvested by lavaging with 4 × 1 ml 0.5 mM EDTA/sterile PBS. Briefly, cells were pelleted; red blood cells (RBC) lysed, washed, and re-suspended; and total recovered lavage cells enumerated using a Coulter counter (Beckman Coulter, Fullerton, CA). Nonspecific antibody binding was blocked by adding purified rat anti-mouse CD16/CD32 (BD PharMingen, San Jose, CA) diluted 1:100 in 30 μg of rat IgG (Jackson ImmunoResearch, West Grove, PA) to each sample before staining with fluorochrome-conjugated antibodies. One microgram of monoclonal antibodies specific to CD11c APC, CD11b PerCp Cy5.5, CD86 FITC, CD54 FITC, Gr-1 APC-Cy7 (BD PharMingen), F4–80 Pacific blue (Caltag Laboratories, Burlingame, CA), or MHC class II PE (eBioscience, San Diego, CA) were added and incubated for 30 minutes on ice. Cells were washed, re-suspended in 0.4 ml PAB (1% bovine serum albumin, 0.01% sodium azide in PBS), and analyzed immediately. Cell acquisition and analysis was performed on a FACS Aria flow cytometer using FACS Diva software (version 4.1.2; Becton Dickinson, Franklin Lakes, NJ). A live cell gate was established using Hoechst 33258 (Invitrogen, Carlsbad, CA) and 100,000 events captured. Compensation of the spectral overlap for each fluorochrome was calculated using anti-rat/hamster Ig compensation beads (BD Biosciences).

In Vivo Labeling of Resident Phagocytic Cells with PKH26 and CD45.1 Monocyte Trafficking

Immediately before intranasal instillation of saline, silica, or titanium dioxide, 100 μl of 15 μM PKH26 (PKH26 Red Fluorescent Phagocytic Cell Linker Kit; Sigma, St. Louis, MO) dissolved in Diluent B was injected intravenously into recipient mice. Three days later, lavage cells were harvested and stained as indicated above. In addition, $CD11b^+$ peripheral blood mononuclear cells (PBMC) were isolated from CD45.1 congenic mice (n = 25). Briefly, PBMC were obtained by cardiac puncture and collection into sterile Eppendorf tubes containing heparin. After RBC lysis and copious washing, cells were pooled together and enumerated using a Coulter counter. Nonspecific antibody binding was blocked as indicated and cells incubated with anti-CD11b magnetic beads and isolated using MACs technology (Miltenyi Biotec, Auburn, CA). Monocyte purity and immunoreactivity for CD45.1 were confirmed by flow cytometry and determined to be ⩾ 85% $CD11b^+$ and ⩾ 95% $CD45.1^+$. Immediately before intranasal instillation of saline or silica, 200 μl of a cell solution containing 10^6 $CD45.1^+$ monocytes was injected intravenously into the tail vein of C57Bl/6 recipient mice. Three days later, lavageable cells were harvested, stained, and analyzed as indicated.

Cell Sorting, Cytokine Enzyme-Linked Immunosorbent Assay, and Microscopic Examination

Lavage cells were obtained from C57Bl/6 mice at 3 days after silica instillation (n = 35–40), and the combined total pooled cells were enumerated using a Coulter counter. Nonspecific antibody binding was blocked, and 1 μg of monoclonal antibody per 10^6 cells specific to CD11c APC (BD PharMingen) and MHC class II (eBioscience) was added and incubated for 30 minutes at 4°C. Cells were washed, re-suspended in 2.0 ml sterile 0.5 mM EDTA/PBS, and sterile sorted immediately (FACS Aria). Cell purity was determined to be ⩾ 85% for AM and DC alike. Replicates of 300,000 AM or DC were plated into microplates with 250 μl of complete RPMI medium and incubated at 37°C for 24 hours. Tissue culture plates were centrifuged and the resulting supernatants collected and analyzed for TNFα, IL-6, and IL-12 production using murine cytokine enzyme-linked immunosorbent assay kits according to the manufacturer's protocol (R&D Systems, Minneapolis, MN).

Preparation of Bone Marrow–Derived Macrophages and DC

In a sterile hood, bone marrow (BM) was aspirated from the femurs and tibias of CD45.1 mice (n = 4) using a 3-ml syringe filled with complete RPMI culture media. Aspirated material was centrifuged, re-suspended in fresh medium, and seeded in tissue culture flasks. After stromal cell elimination by overnight adherence, 20 × 10^6 nonadherent cells were transferred to new flasks including murine M-CSF or GM-CSF (both from R&D Systems) at a final concentration of 20 and 33 ng/ml, respectively. Every third day, the media was boosted with additional growth factor (28) and on Day 5, 8 ml spent media was replaced. By 8 days, cells were fully differentiated, more than 75% confluent, and stained positive for macrophage (Mø) ($F4–80^+$, MHC class II^{lo}) or DC ($CD11c^{hi}$, MHC class II^{hi}) characteristics, confirming appropriate derivation. Viability was determined to be greater than 90% by Trypan blue exclusion staining.

In Vivo Trafficking of BM-Derived Cells and Lymphocyte Activation

Isolation of the BM-derived Mø (BMMø) and BM-derived DC (BMDC) required light scraping and trituration to recover adherent cells from the flask. Cells were washed twice in PBS/EDTA, counted, and viability established. BMMø and BMDC were exposed to crystalline silica in suspension at 100 μg/ml/10^6 live cells for 1 hour. After careful washing to remove excess particle, C57Bl/6 recipient mice (n = 4) were anesthetized with ketamine and intranasally instilled with either 2 × 10^6 BMMø or 2 × 10^6 BMDC suspended in 25 μl of sterile saline. Seventy-two hours later, recipient mice were subjected to lung lavage (indicated above) and lung digest (*see below*).

Preparation of Lung Cell Suspensions

Lungs were ascetically removed, minced into small pieces, and incubated in complete RPMI containing 1 mg/ml collagenase IA (Sigma) at 37°C for approximately 90 minutes. Digested lungs were further disrupted by gently pushing the tissue through a 70-μm cell strainer (BD Biosciences). Enzymatic action was terminated by adding excess complete RPMI and centrifugation. White cells were isolated by centrifugation over a 40 to 70% Percoll gradient (25), enumerated, and a total of 10^6 cells stained for flow cytometry. Initial antibody staining groups were for APC: CD45.1

Pacific Blue (BioLegend, San Diego, CA), CD11c APC, CD11b PerCp Cy5.5, CD86 FITC (BD PharMingen), and MHC class II PE (eBioscience); or for T lymphocytes: CD3 FITC, CD4 APC-Cy7, CD25 PerCp Cy5.5, and CD44 APC (BD PharMingen).

Statistical Analysis

For each parameter, the values for individual mice were averaged and the SD and SE calculated. The significance of the differences between the exposure groups was determined by *t* test, one-way, or two-way ANOVA, in conjunction with Bonferroni's *post hoc* analysis and Tukey's test for variance, where appropriate. All ANOVA models were performed with Prism software, version 4 (GraphPad Software, San Diego, CA). A P value of < 0.05 was considered significant.

RESULTS

CD11c^{hi} Lavage Cells Contain Two Populations of APC

AM and DC may be defined according to expression of combinations of discrete surface markers (7, 29–31). To differentiate between AM and DC, individual mouse lungs were lavaged, and the cells collected, stained with the prescribed cell surface markers, and analyzed using flow cytometry. Naïve C57Bl/6 mice contain a mean $0.569 \pm 0.04 \times 10^6$ live cells, with $87.8 \pm 0.9\%$ of these expressing high levels of CD11c (CD11c^{hi}). Additional gating on dot plots of major histocompatibility complex II (MHC class II) expression versus forward scatter (FSC) revealed two distinct subsets of APC within the CD11c^{hi} lavage cells (Figure 1). For the purposes of this study, MHC class II^{lo} cells were defined as AM, while MHC class II^{hi} cells were defined as DC (30, 31). In naïve C57Bl/6 mice, the vast majority of CD11c^{hi} cells were AM ($98.2 \pm 0.2\%$), while DC constituted a much smaller fraction ($1.7 \pm 0.2\%$) of the lavageable cells. Interestingly, the ratio of AM to DC was noticeably altered in response to crystalline silica (Figure 1B) compared with naïve mice (Figure 1A). Moreover, there was an increase in the median fluorescence intensity (MFI) of CD11b, as well as the appearance of a CD11b^{hi} subset of AM in response to silica (Figure 1B), indicating either phenotypic activation of resident AM or cellular recruitment. Similar observations were made by Kirby and coworkers using a mouse model of pneumoccocal challenge, which demonstrated that CD11b regulates recruitment of AM, but not pulmonary DC (32). These data suggest that an interactive relationship exists between AM and DC within the alveolar spaces during the immune response to crystalline silica.

Because nonmonocytic cells express low levels of CD11c, these cells were excluded from the flow cytometry analysis (Figure 1). Infiltrating monocytes were previously characterized as CD11c$^{lo/negative}$ and CD11b^{positive}, and are defined in this study accordingly (7). CD11b$^+$/Gr-1$^+$/CD11c^{lo} granulocytes constitute less than or equal to 2.5% of the total recovered lung lavage from naïve mice, which confirms a lack of inflammation in naïve mice (Figure 1A). In contrast, crystalline silica resulted in large numbers of CD11b$^+$/Gr-1$^+$/CD11c^{lo} inflammatory cells entering the alveolar spaces 3 days after instillation (Figure 1B). Thus, our model of crystalline silica exposure induces a characteristically strong inflammatory response in C57Bl/6 mice, with CD11b$^+$/Gr-1$^+$/CD11c^{lo} granulocytes entering the alveolar spaces.

Phenotypic Differences between AM and Pulmonary DC

Additional cell surface markers may be used to further differentiate AM and DC (6, 29, 33). Before assessment of the effect that crystalline silica exposure has on AM and DC activation, CD11c^{hi} populations were characterized more extensively with regards to parameters including CD11b, CD86, CD54, F4–80, and side scatter (SSC) properties (indicative of size and granularity). In naïve C57Bl/6 mice, the MFI of CD11b, CD54, and CD86 were significantly elevated on DC compared with AM. Although two distinct subsets of CD11b^{hi} and CD11b^{lo} DC were readily observed, AM were uniformly CD11b^{lo} (histogram not shown). In contrast, the expression of F4–80, a monocytes/macrophage marker, was significantly higher on AM than DC (34). AM and DC may also be distinguished based on size and granularity as estimated by SSC properties (Table 1). Finally, sorted CD11c^{hi}

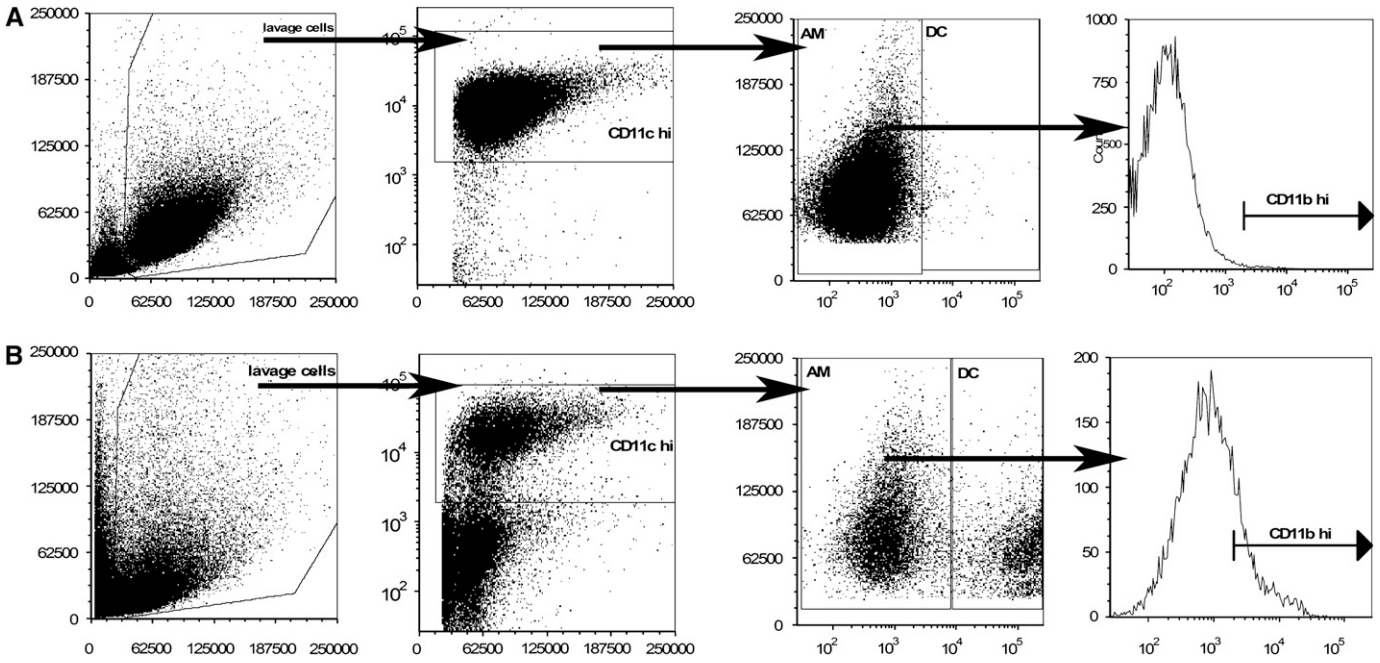

Figure 1. Lung lavage cells from C57Bl/6 mice exposed to saline, silica, or titanium dioxide were examined by flow cytometry and shown to contain both alveolar macrophages (AM) and dendritic cells (DC) within the CD11c^{hi} population. The ratio of AM to DC was altered by silica (*B*) but not saline exposure (*A*). Increases in CD11b mean fluorescence intensity (MFI), and the appearance of CD11b^{hi} AM after silica exposure, suggests shifts in AM phenotype. $n = 4$–6; in duplicate or triplicate.

TABLE 1. CD11c^{hi}-POSITIVE CELLS FROM THE LUNG LAVAGE OF NAÏVE C57BL/6 MICE CONTAINS TWO POPULATIONS OF ANTIGEN-PRESENTING CELLS

Antibody/ Measurement	Fluorescence Conjugation	Alveolar Macrophages (*MFI*)	Dendritic Cells (*MFI*)
F4-80	(Pacific Blue)	225.4 ± 16.63***	43.60 ± 2.249
MHC class II	(PE)	2064 ± 151.3	80370 ± 1,870***
CD11b	(PerCP Cy5.5)	453.2 ± 36.75	1261 ± 194.6**
CD54	(FITC)	297.0 ± 13.50	616.0 ± 52.77**
CD86	(FITC)	615.0 ± 47.73	958.2 ± 37.51***
SSC	N/A	48,880 ± 782.0***	26,640 ± 226.3

Definition of abbreviation: MFI, mean flourescence intensity; SSC, side scatter.

MHC class II^{lo} cells and CD11c^{hi} MHC class II^{hi} cells exhibited the distinct morphologic characteristics of AM and DC, respectively (data not shown). Collectively, these parameters are consistent with the current definition of CD11c^{hi} lavage cells as either AM or DC (7, 20, 33, 34). For the remainder of this study, which investigates the response of AM and DC after silica exposure *in vivo*, a stringent definition of the two cell types was applied by considering CD11c^{hi} MHC class II^{lo} cells as AM and CD11c^{hi} MHC class II^{hi} cells as DC.

Kinetics of APC Distribution after Silica Exposure

Cells isolated from the alveolar spaces were analyzed by flow cytometry to track changes in the percent, absolute number, and ratio of AM to DC at 1, 3, 7, 14, and 28 days after saline, silica, or titanium dioxide (nonfibrogenic particle control) instillation in an established *in vivo* model system (35, 36). No statistical change was observed in the percent of AM or DC in response to either saline or the nonfibrogenic control particle, titanium dioxide (data not shown). In contrast, as shown in Figure 2, gated CD11c^{hi} cells were separated into AM and DC based on MHC II versus FSC expression, and revealed a concomitant loss of AM and gain of DC over time in response to crystalline silica. During the acute phase of the response (Days 1–7), the AM subset of CD11c^{hi} APC declined and returned to baseline levels by 28 days after exposure. This response was mirrored by an opposing reaction within the DC population, which increased during the acute response and also returned to baseline levels by 28 days after exposure (Figure 2).This reciprocal relationship between AM and DC (which collectively make up the CD11c^{hi}

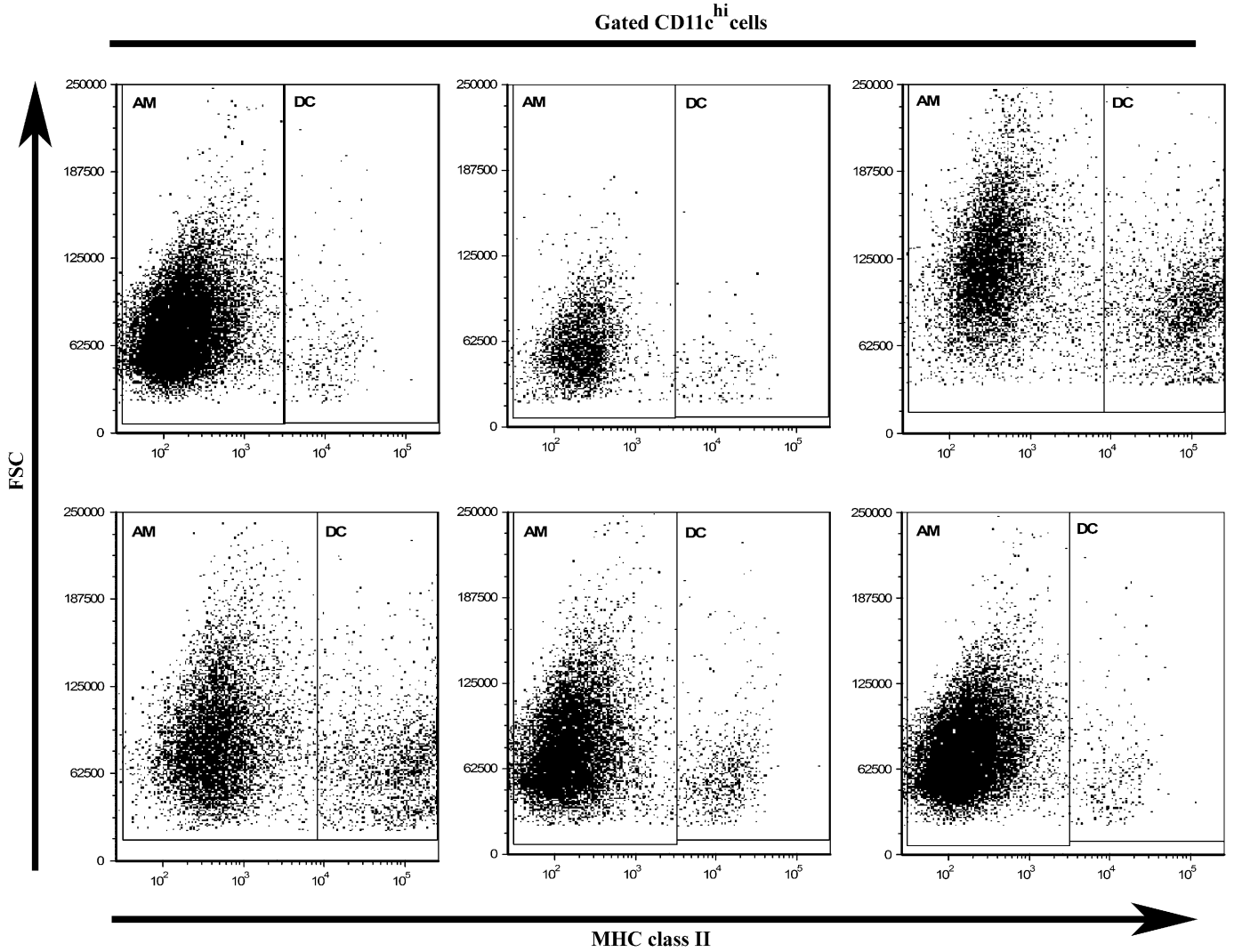

Figure 2. An inverse relationship exists between AM and DC within the lung lavage. Dot plots of forward scatter versus MHC class II expression gated on CD11c^{hi} lavage cells demonstrated that the proportion of cells defined as AM decreases, whereas the proportion defined as DC increases. n = 4–6; in duplicate or triplicate.

population) was most obvious at 3 and 7 days after silica exposure. These data are consistent with previously published reports which demonstrated that AM depletion results in subsequent DC accumulation (31). Accordingly, AM reduction and DC recruitment appear to be in balance after silica exposure.

To determine whether differences in the proportion of CD11c^{hi} cells that were AM versus DC resulted in corresponding shifts in the absolute number, as well as the ratio between AM and DC, additional calculations were performed. As demonstrated in Table 2, AM and DC exhibit distinct kinetics after silica exposure. Consistent with previous reports from our laboratory (25), crystalline silica exposure resulted in a significant decrease in the absolute number of CD11c^{hi} cells, although the total number of recovered lavage cells significantly increased (Table 2)—which may be largely attributed to a pronounced recruitment of inflammatory cells (11, 37, 38). The combined effect of significant decreases in CD11c^{hi} cells and an altered proportion of AM and DC within this population resulted in a profound and significant decline in the absolute number of AM, and a subsequent significant increase in the absolute number of DC (Table 2). Although the most profound reduction in the absolute number of AM occurred between 1 and 3 days, the greatest expansion of DC transpired between 3 and 7 days after silica exposure, suggesting that the kinetics of AM depletion and DC recruitment differ. Furthermore, these data support the notion of an interconnecting relationship between AM and DC dynamics.

In addition, over time, the ratio of AM to DC underwent a robust decline from 34.3 (1 d), to 8.19 (3 d), to 9.49 (7 d), to 21.43 (28 d) in comparison to the full range of ratios (41–150; overall mean equals 79.52) observed in saline exposed mice from all times analyzed (Table 2). Taken together, these results suggest that the presence of DC within the alveolar spaces is inversely related to the presence of AM, and that silica profoundly alters the proportion of CD11c^{hi} cells that are suppressive AM in favor of stimulatory DC.

DC Are Absent from the Lung Lavage of Silica-Exposed Gld and TNFR 1/2–Null Mice

To determine whether the observed reductions in AM and increases in DC are dependent on silica induced AM apoptosis *in vivo*, CD11c^{hi} lavageable cells were examined in TNFR 1/2–null and FasL-deficient (Gld) mice after saline, silica, or titanium dioxide exposure. Neither TNFR 1/2–null nor FasL mice differed from C57Bl/6 wild type with regard to the distribution of cell types within the alveolar spaces of naïve untreated mice (data not shown). Silica triggers events that result in AM apoptosis, and subsequent AM elimination promotes a relative increase in the proportion of CD11c^{hi} cells that are DC, as evidenced by Table 2. Therefore, the balance between AM and DC should remain unchanged in TNFR 1/2–null and FasL-deficient mice in which AM do not undergo apoptosis after silica exposure *in vivo* (39–44). Indeed, neither TNFR 1/2–null nor FasL-deficient mice deviated from saline control in either the percent or absolute number (data not shown) of AM and DC 3 days after crystalline silica exposure. These data provides indirect evidence of the role AM apoptosis may play in the emergence of DC within the alveolar spaces in response to crystalline silica.

Origin of CD11b^{hi}-Positive AM Subpopulation in Silica-Exposed Mice

Initial evaluations of AM phenotype shown in Figure 1 demonstrated an increase in the MFI of CD11b, as well as the occurrence of a CD11b^{hi} AM subset in response to silica. To reveal whether this phenotype is transient or permanent, the frequency of CD11b^{hi} AM was examined over time. No significant change was observed in the percent of CD11b^{hi} AM after either saline (Figure 3A) or titanium dioxide (data not shown). However, a significant increase in CD11b^{hi} AM was observed after crystalline silica exposure compared with saline (Figure 3A), which peaked at 3 days, suggesting that this phenotypic response is specific to silica, and is transient and not permanent.

Subpopulations of AM may be explained by modification of resident AM phenotype or infiltration of cells that represent the altered phenotype. To resolve whether CD11b^{hi} AM are resident cells with an altered phenotype or arise from infiltrating PBMC, two complementary experimental methods were used: adoptive transfer of CD45.1^{+} PBMC into saline- or silica-exposed C57Bl/6 recipient mice, and *in vivo* labeling of tissue resident phagocytic cells by the use of the fluorescent tracer dye PKH26 in saline- and silica-exposed C57Bl/6 mice (45, 46). The adoptive transfer model demonstrated a 2-fold increase in the percent of CD45.1^{+} CD11b^{hi} AM from 45.7 ± 2.4 in the saline-exposed recipient mice to 97.4 ± 1.8 in the silica-exposed recipient mice. Furthermore, a significant increase in the absolute number of CD45.1^{+} CD11b^{hi} AM (Figure 3B) was observed, suggesting that the CD11b^{hi} AM subpopulation principally originated from newly recruited peripheral monocytes. These data also provide novel insight into the inflammatory versus constitutive trafficking of PBMC into the alveolar spaces.

If CD11b^{hi} AM were derived from monocyte precursors in response to silica, experiments that make use of the lipophillic intravaital dye, PKH26, to discriminate resident AM from newly recruited monocytic cells should reveal a decrease in not only the percentage of lavage cells that were PKH26 positive, but also in the MFI of PKH26^{+} cells in response to silica-induced inflammatory conditions (45, 47, 48). In naïve mice, 99.1 ± 0.3% of AM were PKH26^{+}, whereas 96.2 ± 1.3% of CD11b^{hi} AM were PKH26^{+}. Although these values were not altered by saline exposure, a significant decrease was observed in the percent (Figure 3C) and absolute number (data not shown) of PKH26^{+} CD11b^{hi} AM in response to crystalline silica exposure. Further, a significant decrease was observed in the MFI of PKH26^{+} CD11b^{hi} AM from silica- compared with saline-exposed mice (Figure 3D). Taken together, these data indicate that CD11b^{hi} AM principally originated from newly recruited peripheral monocytes and support the notion that during accelerated cell turnover, AM are replenished from newly recruited peripheral cells.

TABLE 2. COMPARISON OF THE ABSOLUTE NUMBER OF CD11c^{hi} CELLS, ALVEOLAR MACROPHAGES, AND DENDRITIC CELLS FROM SALINE- AND SILICA-EXPOSED C57BL/6 MICE

Days	CD11c^{hi} cells (× 10^4)		Alveolar Macrophages CD11c^{hi}, MHC II^{lo} (× 10^4)		Dendritic Cells CD11c^{hi}, MHC II^{hi} (× 10^4)	
	Saline	Silica	Saline	Silica	Saline	Silica
1	31.5 ± 4	6.0 ± 2***	31.2 ± 4	5.5 ± 0.01***	0.24 ± 0.07	0.16 ± 0.04
3	33.6 ± 4	6.6 ± 2***	33.2 ± 4	5.9 ± 0.02***	0.38 ± 0.07	0.72 ± 0.32*
7	21.4 ± 3	10.3 ± 3*	21.1 ± 3	9.4 ± 0.02*	0.36 ± 0.04	0.99 ± 0.27*
28	26.2 ± 2	14.1 ± 2**	25.6 ± 1	13.5 ± 0.02**	0.62 ± 0.09	0.63 ± 0.02

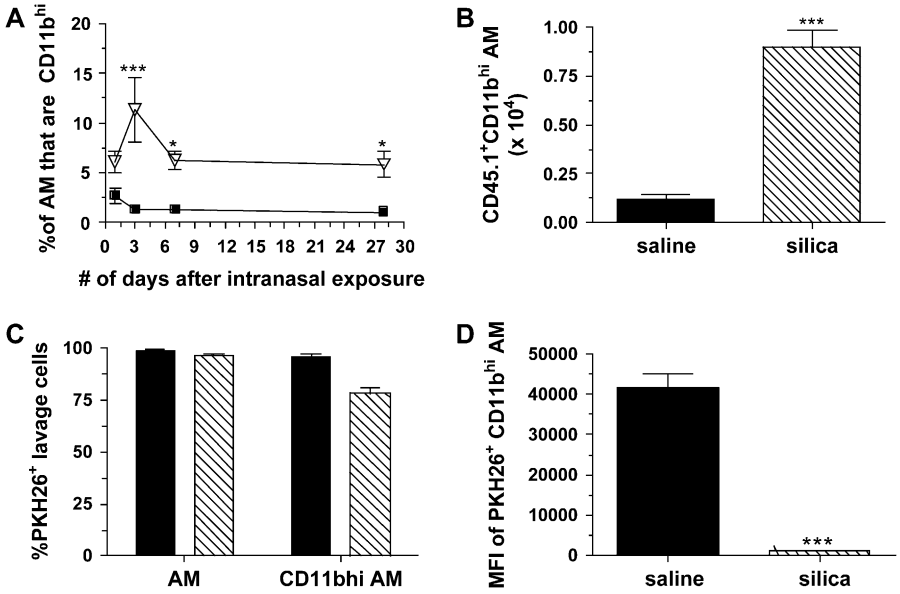

Figure 3. CD11b^{hi} AM principally originated from newly recruited peripheral blood mononuclear cells. (*A*) The percent of CD11b^{hi} AM was significantly increased at 3, 7, and 28 days after silica (*inverted triangles*) compared with saline (*squares*) exposure. (*B*) A significant increase was observed in the absolute number of CD11b^{hi} AM that are CD45.1^{+} after adoptive transfer of monocytes and subsequent silica exposure. (*C*) A significant decrease in the percent of CD11b^{hi} PKH26^{+} AM was observed in silica- but not saline-exposed mice. (*D*) The MFI of PKH26^{+} CD11b^{hi} AM showed a significant reduction of PKH26 MFI. n = 4–6; in duplicate or triplicate. *Error bars* indicate the SEM.*$P < 0.05$, ***$P < 0.001$. *B–D*: *Solid bars*, saline; *hatched bars*, silica.

AM versus DC Activation in Response to Silica Exposure

By analyzing MHC class II, CD11b, CD54, and CD86 MFI while gating specifically on AM and DC, the activation and maturation state of the two cell populations were assessed after particle exposure. The original MFI data obtained from the flow cytometer was transformed into percent of saline control to accommodate both sets of divergent data on the same graph. In this way the response of either AM or DC to silica could be compared with their respective saline control, and the two cell types could be compared with each other. Interestingly, while AM significantly increased MHC class II expression, DC significantly decreased MHC class II expression compared with the appropriate cell-specific saline control; although in both cell types expression of MHC class II returned to baseline by 28 days (Figure 4A). Silica resulted in significantly increased CD11b MFI on AM at 1, 3, and 7 days, yet DC only showed a significant increase in CD11b on Day 7 compared with saline (Figure 4B). The MFI of CD54 was significantly increased on AM after silica exposure compared with saline control at all time points examined, consistent with previous reports (49). In contrast, only at 1 day was CD54 MFI on DC was significantly increased compared with its saline control (Figure 4C). Neither AM nor DC altered CD86 expression after saline, silica, or titanium dioxide exposure (data not shown). Taken together, these data show that AM and DC respond dissimilarly with regard to activation and maturation, suggesting that APC responses to silica are not uniform.

Cytokine Production by AM and DC

To assess the relative contribution of AM and DC to cytokine production, C57Bl/6 mice were exposed to silica and allowed to recover for 3 days before collection of the lavageable cells. After 24 hours in culture, sterile sorted silica-exposed AM secreted significantly more TNF-α, yet less IL-6 than DC. Although DC produced measurable levels of IL-12, those of AM were below the

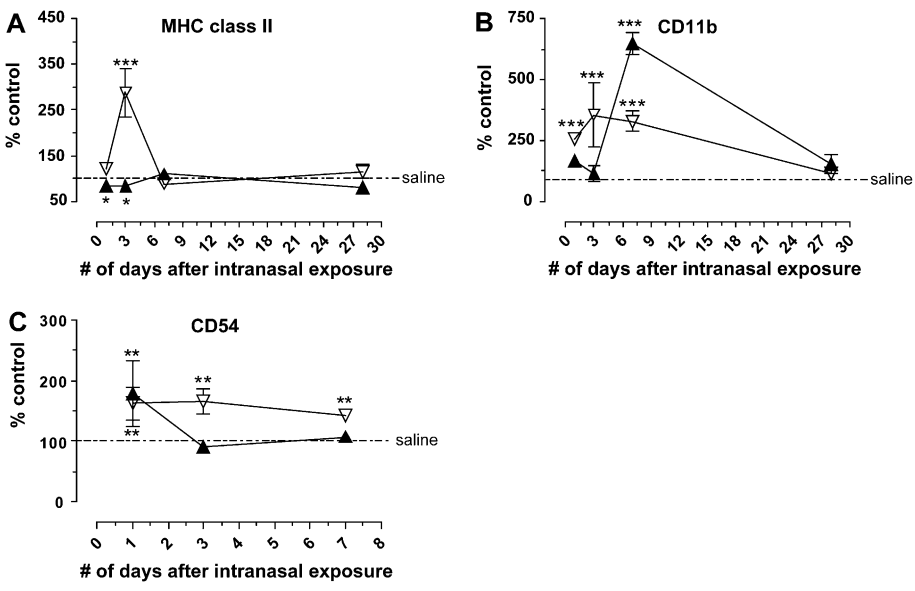

Figure 4. AM (*open inverted triangles*) and DC (*solid triangles*) were activated in response to crystalline silica compared with their respective saline controls. (*A*) Silica significantly increased MHC class II expression on AM compared with the AM saline control at 3 days, yet significantly decreased MHC class II expression below the appropriate DC saline control at 1 and 3 days; although in both MHC class II returned to baseline by 28 days. (*B*) Silica significantly increased CD11b expression on AM at 1, 3, and 7 days compared with the appropriate saline control. In contrast, silica exposure resulted in a transient but significant increase in CD11b expression on DC at 7 days compared with the DC saline control. (*C*) As previously described, CD54 was significantly increased on AM at all time points after silica exposure. In contrast, CD54 on DC is only significantly increased over DC saline control values at 1 day. n = 4–6; in duplicate or triplicate. *Error bars* indicate the SEM. *$P <$ 0.05, **$P < 0.01$, ***$P < 0.001$ compared with the appropriate saline control.

limits of detection (Figure 5). From these findings, it is apparent that silica-induced AM and DC may influence innate and/or humoral respiratory immunity by altering cytokine profiles.

Migration of BMMø versus BMDC

To determine the migratory capacity of APC from the alveolar spaces into the interstitium, BMMø or BMDC derived from bone marrow progenitors of CD45.1 congenic mice were incubated with saline or silica *in vitro* for 1 hour, and subsequently instilled intranasally into C57Bl/6 recipient mice. Derivation of Mø and DC was confirmed by cell surface marker expression and demonstrated that greater than or equal to 95% of cells were $CD45.1^+$ after 8 days in culture (data not shown). Three days after instillation, no difference was observed in the absolute number of $CD45.1^+$ BMMø recovered from the lung lavage or interstitium between recipient mice receiving saline- or silica-treated BMMø (Figure 6A). The recovery rates from the lung lavage of mice receiving saline- and silica-treated $CD45.1^+$ BMMø were 15.4% and 19.7%, respectively, whereas the recovery rates from the interstitium were 5.5% and 4.2%, respectively. These data show that approximately 20 to 25% of the total number of instilled treated $CD45.1^+$ BMMø were recovered, suggesting that the majority of the instilled BMMø are eliminated irrespective of particle treatment. Moreover, no statistical difference in the absolute number of $CD3^+/CD4^+$ interstitial lymphocytes was observed (Figure 6A). In contrast, the absolute number of $CD45.1^+$ BMDC recovered from the lung lavage of recipient mice receiving silica-treated cells was significantly decreased compared with mice receiving saline-treated cells (Figure 6B), with corresponding recovery rates of 55.7% (saline) and 18.4% (silica) of the total number of instilled cells, respectively. Further, the absolute number of $CD45.1^+$ BMDC isolated from the interstitium of mice receiving silica-treated BMDC was significantly increased compared with mice receiving saline-treated BMDC (Figure 6B), with recovery rates of 2.9% (saline) and 5.6% (silica). These data showed that approximately 59% of the total number of saline- and approximately 24% of the total number of silica-treated $CD45.1^+$ BMDC that were instilled were recovered. Collectively, these results indicate that BMMø and BMDC were both susceptible to silica-induced apoptosis and that portions of the original cells were either eliminated or migrated from the airspaces. Finally, the absolute number of $CD3^+/CD4^+$ interstitial lymphocytes was significantly increased in mice receiving silica- compared with saline-treated BMDC (Figure 6B). By instilling saline-and silica-treated BMDC, these results demonstrate that it is not the presence of free silica, but rather the silica-exposed cells themselves that result in increased lymphocyte numbers. These results indicate that DC may play a more important role than previously realized in transporting silica from the bronchoalevolar lumen to the interstitial spaces, and potentially the draining lymph nodes, where they might have fruitful interact with lymphocytes.

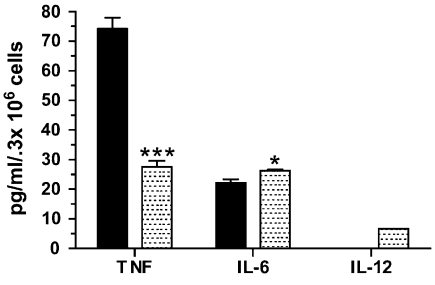

Figure 5. AM (*solid bars*) and DC (*shaded bars*) from silica-exposed mice produced inflammatory cytokines. After 24 hours in culture, sterile sorted silica-exposed AM secreted significantly more TNF-α and significantly less IL-6 than DC. Although DC produced measurable levels of IL-12, AM levels were below the limits of detection. *Error bars* indicate the SEM. $n = 35$–40 pooled, in duplicate. $^*P < 0.05$, $^{***}P < 0.001$.

DISCUSSION

Regulation of pulmonary immune response is a complex process that involves maintaining tolerance to endogenous self-antigens and innocuous environmental particulates, while preserving the ability to appropriately respond to invading microorganisms and pathogens. Respiratory injury perturbs immune homeostasis by inducing an initial inflammatory response, followed by a compensatory anti-inflammatory response. The relative importance of the altered reactivity of these two systems in immune dysfunction observed in respiratory diseases is not yet defined, and remains a subject of some controversy. To begin to understand the balance between immune responses, the purpose of this study was to define the kinetics and activation of AM and pulmonary DC in an *in vivo* model of silicosis.

DC are far superior APC to AM and provoke powerful immune responses, while in contrast, AM appear as weak stimulators or immunosuppressive. Although AM and DC both localize within the alveolar spaces and each performs key functions of innate and adaptive immunity, it is critical to clearly discriminate between the two. Neither cell type may be identified based on the expression of a single cell surface antigen. Rather, a combination of cell surface markers is necessary, which has been shown at a minimum to include CD11c and MHC class II or autofluorescence (14, 31, 33). In this study, AM and DC were discriminated using CD11c and MHC class II, and this definition was confirmed by supplementary cell surface antigens. Using combinations of markers to differentiate AM from DC is advantageous in terms of the ability to discriminate AM and DC without lengthy *in vitro* purification protocols, as well as fluorescent channel occupation and the ability to examine additional markers of interest using multicolor flow cytometry.

Recruitment of immune cells is a prominent feature of respiratory inflammation and a prototypical response to environmental pathogens. After silica exposure, our results demonstrated that there is a significant decrease in the percent and absolute number of AM, and a subsequent significant increase in the percent and number of DC that takes place over time. The loss of AM and gain of DC suggests that under normal physiologic conditions AM may be an important prerequisite for the down-regulation of respiratory immunity to maintain immune homeostasis. AM-mediated suppression of DC activity and function results from the secretion of soluble factors and/or cell–cell contact—although the exact mechanism remains unknown. When AM-mediated suppression is abrogated by clodronate treatment or silica-induced apoptosis, significant increases in the presence and activity of DC may result in enhanced presentation of antigens, T cell activation, and increased immune responses. Therefore, perturbation of the balance between immunosuppressive and immunoenhancing APC by silica may result in immune instability, inflammation, and fibrosis (14).

Previous studies from our laboratory and others have shown that exposure to silica *in vivo* and *in vitro* induces apoptosis of AM, and that both Fas-FasL and TNF-α play important roles in this process (10, 39, 42, 50). Neither TNFR 1/2–null nor FasL (Gld)-deficient mice exhibited any change in the percent or absolute number of AM and DC after silica exposure, providing indirect evidence supporting the notion that AM apoptosis may be necessary to initiate the influx of pulmonary DC into the alveolar spaces. Alternatively, the observed reductions shown in recovered AM may occur as a result of increased cellular

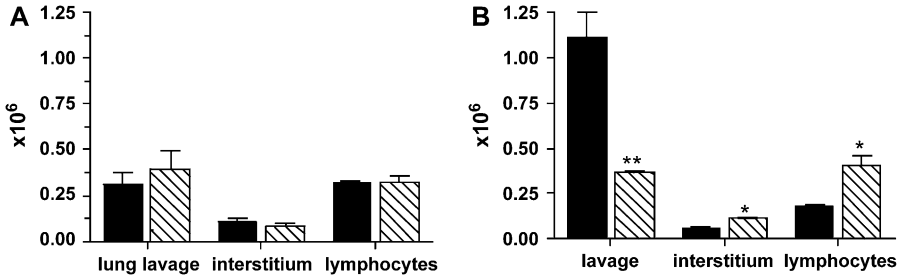

Figure 6. Bone marrow–derived macrophages (BMMø) and DC (BMDC) from CD45.1 mice were treated with silica *in vitro* for 1 hour and instilled intranasally into recipient mice. (*A*) No difference was observed in the absolute number of CD45.1$^+$ BMMø recovered from the lavage or interstitium, nor in the absolute number of CD3$^+$/CD4$^+$ interstitial lymphocytes. (*B*) The absolute number of CD45.1$^+$ cells recovered from mice receiving silica-treated BMDC was significantly decreased compared with saline. In contrast, the absolute number of CD45.1$^+$ cells recovered from the interstitium of mice receiving silica-treated BMDC was significantly increased compared with saline. A significant increase in the absolute number of CD3$^+$/CD4$^+$ lymphocytes was detected in mice receiving silica-exposed BMDC compared with saline. $n = 3$–4; in duplicate. *Error bars* indicate the SEM. *$P < 0.05$, **$P < 0.01$, ***$P < 0.001$. *Solid bars*, saline; *hatched bars*, silica.

migration into the parenchyma of the lung and cell excretion via the mucociliary escalators. In addition, because TNF-α may initiate inflammatory cell recruitment by promoting up-regulation of cell adhesion molecules and chemokines, it is plausible that in TNFR 1/2–null mice not only is silica-induced apoptosis suppressed, but also inflammatory cell recruitment and migration.

Not only were the ratios of AM to DC dramatically altered after silica exposure, but also AM and DC phenotype. A significant increase in the percent of CD11b^{hi} AM was observed and these cells were shown by two complimentary methods to predominantly arise from PBMC. Previous studies demonstrated infectious agents induce monocyte recruitment to the alveolar spaces (51) and that resident tissue Mø are replenished by constitutive cellular turnover within defined rates (48). These freshly recruited monocytes are largely proinflammatory, display phagocytotic poperties, and promote rather than inhibit lymphocyte and DC activation. Therefore, there may actually be three populations of APC present within the alveolar spaces: resident immunosuppressive AM, infiltrating immune active monocytes, and pulmonary DC. Acquisition of the immunosuppressive phenotype of AM by monocytes requires time, allowing a brief window of opportunity for launching innate and adaptive immunity (18, 52). The presence of DC during this window of opportunity may have significant impacts on innate (inflammatory) and adaptive (pro-fibrotic) immunity.

A major function of APC is ingestion of foreign particles and debris, subsequent digestion, and in some instances presentation of the foreign Ag in conjunction with MHC class II. AM and DC ingest and interact with silica based on changes in side scatter profiles (data not shown), and these interactions result in unique activation patterns as measured by changes in cell surface markers. DC express the scavenger receptor MARCO, and previous studies from our laboratory demonstrated that MARCO mediates silica uptake and toxicity in AM from C57Bl/6 mice *ex vivo* (36, 53, 54) and that MARCO expression on BMDC correlates with silica uptake (data not shown). To our knowledge, this study represents the first analysis of DC interactions with and response to crystalline silica *in vivo*.

It is likely that AM- and DC-derived cytokines modulate innate and adaptive immununity. Using the FACS Aria system to sterile sort AM from DC, we have demonstrated that both cells secrete TNF-α after silica exposure and 24 hours in culture; however, TNF-α production by AM is significantly increased compared with DC. In contrast, DC-derived production of IL-6 and IL-12 is significantly increased compared with AM. Silica-induced production of cytokines by Mø may induce the maturation of DC (55), and AM-derived TNF-α may be responsible for DC recruitment and activation. In contrast, DC production of IL-6 and IL-12 may influence distinct steps in the adaptive immune response (56). Although the purity of AM and DC cultures were determined to be greater than or equal to 85% after sorting, one cannot exclude the possibility of cell contamination of one type or the other in the opposing cultures contributing to cytokine production.

For proper initiation of a respiratory immune response, Ag must be transported by APC and subsequently competent interactions with lymphocytes occur via MHC class II and other co-stimulatory molecules. Although such transportation functions have been assigned to AM, it is more likely that DC are responsible for this process (13, 21, 22). Splenic DC pulsed with Ag and instilled into the alveolar spaces induce Ag-specific T cell priming in the mediastinal LN, while AM do not (15, 16, 31). In response to silica, a portion of BMDC and BMMø migrated into the interstitium, although only BMDC subsequently significantly increased the absolute number of CD3$^+$CD4$^+$ lymphocytes. Although the current study did not specifically analyze DC migration into the draining mediastinal lymph nodes (LN), it is known that DC are present in nonlymphoid tissues as immature precursors and process environmental antigens before maturing and migrating to the T cell areas of the draining LN (57), and this process may contribute to the observed decreases in the number of DC recovered.

DC and AM act in opposition to one another with regard to the initiation and maintenance of respiratory inflammation. Whereas lung DC activate lymphocytes and thereby promote immune activation, AM suppress these functions. Therefore, it has been suggested that the balance of these two cells types influences the progression of respiratory inflammation. The results presented in this study provide novel insight into the interactions between crystalline silica and APC *in vivo* and further define the dynamic interaction between AM and DC. Understanding the mechanisms that may restore the balance between immunosuppression and immunoenhancement within the alveolar spaces may lead to novel therapeutic strategies to control respiratory conditions including asthma, autoimmune pulmonary fibrosis, silicosis, and idiopathic pulmonary fibrosis.

Conflict of Interest Statement: None of the authors has a financial relationship with a commercial entity that has an interest in the subject of this manuscript.

References

1. American Thoracic Society committee of the scientific assembly on environmental and occupational health. Adverse effects of crystalline silica exposure. *Am J Respir Crit Care Med* 1997;155:761–768.
2. Parks CG, Conrad K, Cooper GS. Occupational exposure to crystalline silica and autoimmune disease. *Environ Health Perspect* 1999;107: 793–802.
3. Parks CG, Cooper GS, Nylander-French LA, Sanderson WT, Dement JM, Cohen PL, Dooley MA, Treadwell EL, St Clair EW, Gilkeson GS, *et al.* Occupational exposure to crystalline silica and risk of systemic lupus erythematosus: a population-based, case-control study in the southeastern united states. *Arthritis Rheum* 2002;46:1840–1850.

4. Ding M, Chen F, Shi X, Yucesoy B, Mossman B, Vallyathan V. Diseases caused by silica: mechanisms of injury and disease development. *Int Immunopharmacol* 2002;2:173–182.
5. Holt PG, Oliver J, Bilyk N, McMenamin C, McMenamin PG, Kraal G, Thepen T. Downregulation of the antigen presenting cell function(s) of pulmonary dendritic cells in vivo by resident alveolar macrophages. *J Exp Med* 1993;177:397–407.
6. Julia V, Hessel EM, Malherbe L, Glaichenhaus N, O'Garra A, Coffman RL. A restricted subset of dendritic cells captures airborne antigens and remains able to activate specific T cells long after antigen exposure. *Immunity* 2002;16:271–283.
7. Gonzalez-Juarrero M, Shim TS, Kipnis A, Junqueira-Kipnis AP, Orme IM. Dynamics of macrophage cell populations during murine pulmonary tuberculosis. *J Immunol* 2003;171:3128–3135.
8. Delclaux C, Azoulay E. Inflammatory response to infectious pulmonary injury. *Eur Respir J Suppl* 2003;42:10s–14s.
9. Palecanda A, Kobzik L. Receptors for unopsonized particles: the role of alveolar macrophage scavenger receptors. *Curr Mol Med* 2001;1: 589–595.
10. Barbarin V, Nihoul A, Misson P, Arras M, Delos M, Leclercq I, Lison D, Huaux F. The role of pro- and anti-inflammatory responses in silica-induced lung fibrosis. *Respir Res* 2005;6:112.
11. Rimal B, Greenberg AK, Rom WN. Basic pathogenetic mechanisms in silicosis: current understanding. *Curr Opin Pulm Med* 2005;11:169–173.
12. Hamilton RF, de Villiers WJ, Holian A. Class a type II scavenger receptor mediates silica-induced apoptosis in chinese hamster ovary cell line. *Toxicol Appl Pharmacol* 2000;162:100–106.
13. Thepen T, Van Rooijen N, Kraal G. Alveolar macrophage elimination in vivo is associated with an increase in pulmonary immune response in mice. *J Exp Med* 1989;170:499–509.
14. Havenith CE, Breedijk AJ, Hoefsmit EC. Effect of bacillus calmette-guerin inoculation on numbers of dendritic cells in bronchoalveolar lavages of rats. *Immunobiology* 1992;184:336–347.
15. Holt PG. Down-regulation of immune responses in the lower respiratory tract: the role of alveolar macrophages. *Clin Exp Immunol* 1986;63: 261–270.
16. Havenith CE, Breedijk AJ, Calame W, Beelen RH, Hoefsmit EC. Antigen specific T cell priming in vivo by intratracheal injection of antigen presenting cells. *Adv Exp Med Biol* 1993;329:571–575.
17. Webb TJ, Sumpter TL, Thiele AT, Swanson KA, Wilkes DS. The phenotype and function of lung dendritic cells. *Crit Rev Immunol* 2005; 25:465–491.
18. Bilyk N, Holt PG. Cytokine modulation of the immunosuppressive phenotype of pulmonary alveolar macrophage populations. *Immunology* 1995;86:231–237.
19. Bilyk N, Mackenzie JS, Papadimitriou JM, Holt PG. Functional studies on macrophage populations in the airways and the lung wall of spf mice in the steady-state and during respiratory virus infection. *Immunology* 1988;65:417–425.
20. von Garnier C, Filgueira L, Wikstrom M, Smith M, Thomas JA, Strickland DH, Holt PG, Stumbles PA. Anatomical location determines the distribution and function of dendritic cells and other APCs in the respiratory tract. *J Immunol* 2005;175:1609–1618.
21. Harmsen AG, Muggenburg BA, Snipes MB, Bice DE. The role of macrophages in particle translocation from lungs to lymph nodes. *Science* 1985;230:1277–1280.
22. Lehnert BE, Valdez YE, Stewart CC. Translocation of particles to the tracheobronchial lymph nodes after lung deposition: kinetics and particle-cell relationships. *Exp Lung Res* 1986;10:245–266.
23. Thepen T, Kraal G, Holt PG. The role of alveolar macrophages in regulation of lung inflammation. *Ann N Y Acad Sci* 1994;725:200–206.
24. Leemans JC, Juffermans NP, Florquin S, van Rooijen N, Vervoordeldonk MJ, Verbon A, van Deventer SJ, van der Poll T. Depletion of alveolar macrophages exerts protective effects in pulmonary tuberculosis in mice. *J Immunol* 2001;166:4604–4611.
25. Migliaccio CT, Hamilton RF Jr, Holian A. Increase in a distinct pulmonary macrophage subset possessing an antigen-presenting cell phenotype and in vitro APC activity following silica exposure. *Toxicol Appl Pharmacol* 2005;205:168–176.
26. Vanhee D, Gosset P, Boitelle A, Wallaert B, Tonnel AB. Cytokines and cytokine network in silicosis and coal workers' pneumoconiosis. *Eur Respir J* 1995;8:834–842.
27. Lalmanach G, Diot E, Godat E, Lecaille F, Herve-Grepinet V. Cysteine cathepsins and caspases in silicosis. *Biol Chem* 2006;387:863–870.
28. Pfau JC, Schneider JC, Archer AJ, Sentissi J, Leyva FJ, Cramton J. Environmental oxygen tension affects phenotype in cultured bone marrow-derived macrophages. *Am J Physiol Lung Cell Mol Physiol* 2004;286:L354–L362.
29. Landsman L, Varol C, Jung S. Distinct differentiation potential of blood monocyte subsets in the lung. *J Immunol* 2007;178:2000–2007.
30. Humphreys IR, Stewart GR, Turner DJ, Patel J, Karamanou D, Snelgrove RJ, Young DB. A role for dendritic cells in the dissemination of mycobacterial infection. *Microbes Infect* 2006;8:1339–1346.
31. Jakubzick C, Tacke F, Llodra J, van Rooijen N, Randolph GJ. Modulation of dendritic cell trafficking to and from the airways. *J Immunol* 2006;176:3578–3584.
32. Kirby AC, Raynes JG, Kaye PM. Cd11b regulates recruitment of alveolar macrophages but not pulmonary dendritic cells after pneumococcal challenge. *J Infect Dis* 2006;193:205–213.
33. Vermaelen K, Pauwels R. Accurate and simple discrimination of mouse pulmonary dendritic cell and macrophage populations by flow cytometry: methodology and new insights. *Cytometry A* 2004;61:170–177.
34. Kirby A, Newton D, Carding S, Kaye P. Pulmonary dendritic cells and alveolar macrophages are regulated by γδ T cells during the resolution of *S. pneumoniae*-induced inflammation. *J Pathol* 2007;212:29–37.
35. Beamer CA, Holian A. Scavenger receptor class a type i/ii (cd204) null mice fail to develop fibrosis following silica exposure. *Am J Physiol Lung Cell Mol Physiol* 2005;289:L186–L195.
36. Hamilton RF, Jr., Thakur SA, Mayfair JK, Holian A. Marco mediates silica uptake and toxicity in alveolar macrophages from c57bl/6 mice. *J Biol Chem* 2006.
37. Zhai R, Ge X, Li H, Tang Z, Liao R, Kleinjans J. Differences in cellular and inflammatory cytokine profiles in the bronchoalveolar lavage fluid in bagassosis and silicosis. *Am J Ind Med* 2004;46:338–344.
38. Huaux F. New developments in the understanding of immunology in silicosis. *Curr Opin Allergy Clin Immunol* 2007;7:168–173.
39. Gozal E, Ortiz LA, Zou X, Burow ME, Lasky JA, Friedman M. Silica-induced apoptosis in murine macrophage: involvement of tumor necrosis factor-alpha and nuclear factor-kappab activation. *Am J Respir Cell Mol Biol* 2002;27:91–98.
40. Piguet PF, Collart MA, Grau GE, Sappino AP, Vassalli P. Requirement of tumour necrosis factor for development of silica-induced pulmonary fibrosis. *Nature* 1990;344:245–247.
41. Corsini E, Giani A, Peano S, Marinovich M, Galli CL. Resistance to silica-induced lung fibrosis in senescent rats: role of alveolar macrophages and tumor necrosis factor-alpha (tnf). *Mech Ageing Dev* 2004;125:145–146.
42. Borges VM, Falcao H, Leite-Junior JH, Alvim L, Teixeira GP, Russo M, Nobrega AF, Lopes MF, Rocco PM, Davidson WF, *et al*. Fas ligand triggers pulmonary silicosis. *J Exp Med* 2001;194:155–164.
43. Hagimoto N, Kuwano K, Miyazaki H, Kunitake R, Fujita M, Kawasaki M, Kaneko Y, Hara N. Induction of apoptosis and pulmonary fibrosis in mice in response to ligation of fas antigen. *Am J Respir Cell Mol Biol* 1997;17:272–278.
44. Hagimoto N, Kuwano K, Nomoto Y, Kunitake R, Hara N. Apoptosis and expression of fas/fas ligand mrna in bleomycin-induced pulmonary fibrosis in mice. *Am J Respir Cell Mol Biol* 1997;16:91–101.
45. Maus U, Herold S, Muth H, Maus R, Ermert L, Ermert M, Weissmann N, Rosseau S, Seeger W, Grimminger F, *et al*. Monocytes recruited into the alveolar air space of mice show a monocytic phenotype but upregulate cd14. *Am J Physiol Lung Cell Mol Physiol* 2001;280:L58–L68.
46. Garn H, Siese A, Stumpf S, Wensing A, Renz H, Gemsa D. Phenotypical and functional characterization of alveolar macrophage subpopulations in the lungs of no2-exposed rats. *Respir Res* 2006;7:4.
47. Maus U, Huwe J, Ermert L, Ermert M, Seeger W, Lohmeyer J. Molecular pathways of monocyte emigration into the alveolar air space of intact mice. *Am J Respir Crit Care Med* 2002;165:95–100.
48. Srivastava M, Jung S, Wilhelm J, Fink L, Buhling F, Welte T, Bohle RM, Seeger W, Lohmeyer J, Maus UA. The inflammatory versus constitutive trafficking of mononuclear phagocytes into the alveolar space of mice is associated with drastic changes in their gene expression profiles. *J Immunol* 2005;175:1884–1893.
49. Hubbard AK, Giardina C. Regulation of ICAM-1 expression in mouse macrophages. *Inflammation* 2000;24:115–125.
50. Borges VM, Lopes MF, Falcao H, Leite-Junior JH, Rocco PR, Davidson WF, Linden R, Zin WA, DosReis GA. Apoptosis underlies immunopathogenic mechanisms in acute silicosis. *Am J Respir Cell Mol Biol* 2002;27:78–84.
51. Warmington KS, Boring L, Ruth JH, Sonstein J, Hogaboam CM, Curtis JL, Kunkel SL, Charo IR, Chensue SW. Effect of c–c chemokine receptor 2 (ccr2) knockout on type-2 (schistosomal antigen-elicited)

pulmonary granuloma formation: analysis of cellular recruitment and cytokine responses. *Am J Pathol* 1999;154:1407–1416.
52. Bilyk N, Holt PG. Inhibition of the immunosuppressive activity of resident pulmonary alveolar macrophages by granulocyte/macrophage colony-stimulating factor. *J Exp Med* 1993;177:1773–1777.
53. Milne SA, McGregor AL, McCulloch J, Sharkey J. Increased expression of macrophage receptor with collagenous structure (marco) in mouse cortex following middle cerebral artery occlusion. *Neurosci Lett* 2005;383:58–62.
54. Granucci F, Petralia F, Urbano M, Citterio S, Di Tota F, Santambrogio L, Ricciardi-Castagnoli P. The scavenger receptor marco mediates cytoskeleton rearrangements in dendritic cells and microglia. *Blood* 2003;102:2940–2947.
55. Pernis B. Silica and the immune system. *Acta Biomed Ateneo Parmense* 2005;76:38–44.
56. Steinman RM, Hemmi H. Dendritic cells: translating innate to adaptive immunity. *Curr Top Microbiol Immunol* 2006;311:17–58.
57. Havenith CE, van Miert PP, Breedijk AJ, Beelen RH, Hoefsmit EC. Migration of dendritic cells into the draining lymph nodes of the lung after intratracheal instillation. *Am J Respir Cell Mol Biol* 1993;9:484–488.